I&EC research
Industrial & Engineering Chemistry Research

Article

pubs.acs.org/IECR

Hydrodeoxygenation of Anisole with Pt Catalysts

M. S. Zanuttini, C. D. Lago, M. S. Gross, M. A. Peralta, and C. A. Querini*

Instituto de Investigaciones en Catálisis y Petroquímica (INCAPE) − FIQ − UNL − CONICET, Santiago del Estero 2654, Santa Fe S3000AOJ, Argentina

Supporting Information

ABSTRACT: Pt catalysts supported on neutral and acid materials, namely SiO_2, γ-Al_2O_3, Na-Beta, and NaH-Beta, were studied in the anisole deoxygenation reaction. The main objective was to compare different supports for this reaction and determine the conditions that maximize the selectivity to deoxygenated products. The reactions were carried out in a fixed-bed reactor at atmospheric pressure by varying the temperature between 200 and 500 °C. Depending on reaction conditions, benzene, and in lesser amounts toluene and xylenes, were obtained as deoxygenated products. Also, n-methylanisoles and n-methylphenols were produced in low amounts. The effects of space time, temperature, and H_2/anisole ratio on the catalytic performance were analyzed in a wide range of values, which thus made it possible to obtain detailed information regarding the changes in selectivity and activity upon changes in the operational variables. Anisole deoxygenation to benzene requires both the metallic and the acid functions. Acid and metal sites promoted demethylation needed to allow the deoxygenation reaction to occur. The acid sites also promote transalkylation reactions, which led to undesired oxygenated products, and on the other hand, the acidity catalyzed the alkylation of aromatic rings with the $-CH_3$ fragments coming from demethylation, thus improving the carbon balance. Coke formation follows a series-type mechanism, formed mainly from the anisole. It is possible to regenerate these catalysts by burning the coke with air at 350−400 °C. The catalysts supported on the beta zeolite worked under a mass transfer controlled regime.

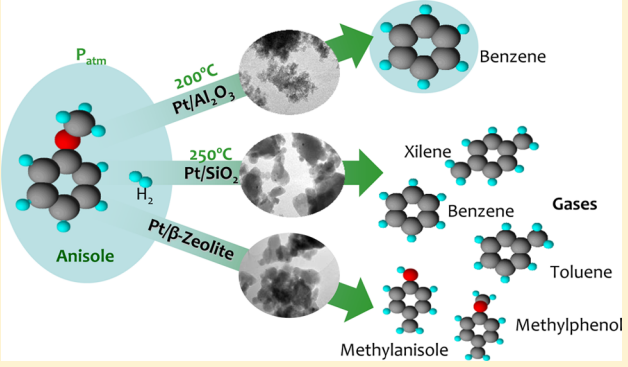

1. INTRODUCTION

Fast pyrolysis of biomass for bio-oil production is a direct route to renewable liquid fuels. To produce liquids hydrocarbons, bio-oil must be upgraded by catalytic hydrotreatment since its high oxygen content imparts negative properties to the fuel. These negative properties are high viscosity, low heating value, corrosiveness, and instability.[1−3] Moreover, the high reactivity complicates the use of bio-oil as a fuel and its long-term storage.

The deoxygenation of different bio-oil model compounds was studied to better understand the reactions involved in the upgrading process. In this work, the deoxygenation of anisole is studied. Silica-supported Ni_2P, MoP, and NiMoP catalysts were studied in the hydrodeoxygenation (HDO) of anisole.[4] Both metal sites ($Ni^{\delta+}$ and $Mo^{\delta+}$) and PO-H groups on phosphides were active for demethylation, hydrogenolysis, and hydrogenation reactions. The metal sites were more active than the PO-H groups. The authors concluded that the disadvantage of these catalysts is that during the anisole HDO, the metal and phosphide may be transformed into metal oxide or phosphate due to the reaction with water, which might cover the metal sites and transform the Lewis acid sites into Brønsted acid sites leading to the deactivation of phosphides catalysts.

The deoxygenation of phenol and cresol were previously studied.[5−7] It was found that the phenol deoxygenation is mostly controlled by the metallic function, although acidity is also required to catalyze the dehydration steps. The Pt/SiO_2 and Pt/γ-Al_2O_3 catalysts were very active and selective for the deoxygenation of cresol to toluene, which is a high octane product. Pt/BEA catalysts were also active although less selective to deoxygenated products and deactivated faster. The deoxygenation of phenol and cresol will be taken as reference since these compounds are reaction intermediates in the anisole deoxygenation reactions. It has been shown that Pt is very selective in the phenol deoxygenation reactions.[5−7] Therefore, it is very important to study the same catalysts to determine if it is possible to obtain good results regarding activity and selectivity to deoxygenated products using anisole as reactant under the same experimental conditions than those find for m-cresol and phenol deoxygenation.

Gonzalez-Borja et al.[8] also stated that a Pt catalyst is active for anisole deoxygenation. They found that the system Pt−Sn/CNF/inconel monolith was able to fully deoxygenate anisole at 400 °C and atmospheric pressure, although its stability was not good. The acid function had positive effects since it promoted alkylation reactions minimizing the carbon loss. It is for this

Received: February 6, 2017
Revised: April 30, 2017
Accepted: May 8, 2017
Published: May 8, 2017

DOI: 10.1021/acs.iecr.7b00521
Ind. Eng. Chem. Res. 2017, 56, 6419−6431

reason that a rational balance between high production of deoxygenated products and low carbon loss must be obtained.

Runnebaum et al.[9] studied the conversion of anisole in the presence of H_2 in a fixed bed reactor at 300 °C and 1.4 bar using platinum on alumina catalysts. More than 40 reaction products were detected by gas chromatography and mass spectroscopy, being the most abundant phenol, 2-methylphenol, benzene, and 2,6-dimethylphenol. Several reactions were identified such as hydrogenolysis, cracking, and transfer of the methyl group.

Nickel is a metal that received particular attention as catalyst for the hydrodeoxygenation of anisole. A recent work of Yang et al.[10] presented results of series of Ni catalysts supported on various materials by analyzing the influence of the metal−support interactions on the selectivity of anisole hydrodeoxygenation. Reaction tests were conducted between 290 and 310 °C at 3 bar. Differences in the product distribution among the catalysts were attributed not only to variations in the dispersion of the metal phase, but also to the influence of the properties of the support. Two main reaction paths for anisole processing were proposed, depending on the configuration of the molecule adsorption. In the case in which the adsorption occurs through the oxygen bond, the demethylation was facilitated, while the adsorption via π-bond leads to the hydrogenation of the aromatic ring. Ni−Cu bimetallic catalysts were evaluated at 280 °C and 6 MPa[11] and found that the main products were cyclohexane and methoxycyclohexane, with very low selectivity to benzene. Catalysts based on nickel impregnated on several supports were evaluated also by S. Jin et al.[12] working at a reaction temperature range of 180−200 °C. It was found that low pressures (0.5−1 MPa) favor the formation of benzene, and at higher pressures, mainly cyclohexane was produced. Low levels of acidity and high Ni dispersion leads to high HDO selectivities. With the objective of improving the Ni selectivity, bimetallic Ni−Co catalysts were also studied,[13] but at high pressure (50 bar) and at 220 °C. Under these conditions, cyclohexane was the main product with very low selectivity to benzene. Ni-based commercial catalysts were used by J.E. Peters et al.[14] in the hydrodeoxygenation of anisole and guaiacol, but at relatively high temperatures, in the range of 350−450 °C. In all cases, use of nickel to deoxygenate anisole pressures above 1 bar is needed to obtain good results.

A Pt/HBEA catalyst was studied in the deoxygenation of anisole[15] at 400 °C. It was found that this catalyst is active for both methyl transfer and hydrodeoxygenation, leading to the formation of benzene, toluene, and xylenes.

CoMoW/SBA-15 catalyst was also studied in the hydroconversion of anisole at 310 °C and 3 MPa. The main products were phenol, cresol, and xylenol, with a very low selectivity to benzene, approximately 1%.[16]

It can be concluded that most of the catalysts were studied at pressures above 1 bar, being the catalysts containing platinum the more selective at this low pressure. Besides, the deactivation mechanism, coke characterization, and regeneration strategies for the anisole hydrodeoxygenation were not reported. This is not only important from a basic point of view to correlate the process variables with the coke amount deposited on the catalyst and its deactivation capacity (i.e., toxicity), but also from an applied point of view to properly select and design catalysts that could be operated for many reaction-regeneration cycles.

In the present work, the anisole deoxygenation is studied using Pt catalysts supported on neutral and acid materials, namely SiO_2, γ-Al_2O_3, Na-Beta, and H-Beta, to compare the effects of different supports having different acidity and porous structure. The acid nature of the Pt/BEA catalysts is modified by exchanging the zeolite with sodium to better understand the role of the acid function in the selectivity and stability of the catalyst since the Pt/HBEA system deactivates relatively fast. The catalyst deactivation and regeneration are also addressed in this study. The catalysts are evaluated in a wide range of temperature, W/F, and H_2/Anisole molar ratios to determine the conditions that maximize the yields of deoxygenated products.

2. EXPERIMENTAL SECTION

2.1. Catalysts Preparation. Tetra-amine platinum(II) nitrate (metal content 50%) supplied by Alfa Aesar, dissolved in water, was used as precursor to prepare the Pt supported catalysts. The amount of the precursor was calculated to obtain a final loading of 1.7 wt % of Pt in each support. Four different supports were used in this work: γ-Al_2O_3 (CK-300, Ketjen), SiO_2 gel (Alfa Aesar), and beta (BEA) zeolites in the protonic and sodic forms. In all cases, a suspension of the support in the metal precursor solution was stirred on a hot plate at 110 °C until complete evaporation. The impregnated catalyst was dried in an oven at 110 °C for 12 h and then calcined at 350 °C for 2 h. The beta zeolite was manufactured by UOP and had a Si/Al ratio of 13. The sodium form of this zeolite was obtained by ion-exchanged using a solution of NaOH (Cicarreli) 0.25 M for 3 h under reflux conditions. Afterward it was filtered and dried at 100 °C and then calcined at 550 °C. The sodium content of this zeolite was 1%. This support was labeled as Na−B. This catalyst was then exchanged with NH_4NO_3 (Anedra) to obtain again the protonic form, to determine if the preparation procedure followed to obtain the Na−B catalyst led to a zeolite structural change. This support was labeled as NaH-B.

The final Pt content on these catalysts was verified by ICP.

2.2. Catalyst Characterization. The porosity was determined from nitrogen adsorption−desorption isotherms, obtained at liquid-nitrogen temperature and relative pressures (P/P_0) between 6×10^{-7} and 0.998 on a Quantachrome equipment. The BET model was used in the relative pressure range 0.01−0.10 to calculate the total surface area. Samples were pretreated under vacuum at 350 °C during 3 h.

X-ray Diffraction (XRD) patterns were carried out with a Shimadzu XD-D1 instrument with monochromator using CuK radiation. The scanning rate used was 4° min^{-1} for Pt(1.7%)/γ-Al_2O_3 and Pt(1.7%)/SiO_2 catalysts, and 0.5° min^{-1} in the case of the Pt(1.7%)/zeolite catalysts. In all cases, the spectra were measured in the range 2θ = 5−100°. Scherrer's equation was used to calculate the crystallite size of Pt and the thickness of the crystal in a direction perpendicular to the (1 1 1) lattice plane.[7]

The metallic particle sizes for Pt/γ-Al_2O_3 and Pt/SiO_2 catalysts were determined by transmission electron microscopy (TEM) using a JEOL 100 CX model microscope at 100 kV and a magnification of 450 000×. The reduced samples were dispersed in distilled water. One drop of this suspension was then placed on holey carbon supported on a copper grid.

Temperature-programmed reduction (TPR) analyses were carried out by heating the sample from 20 to 700 °C at a rate of 11 °C min^{-1}, using a mixture of 5% H_2 in Ar, using a thermal conductivity detector.

DOI: 10.1021/acs.iecr.7b00521
Ind. Eng. Chem. Res. 2017, 56, 6419−6431

The metallic dispersions were calculated based on the H_2 chemisorption isotherms, which were made in volumetric equipment at room temperature, measuring between 25 and 100 Torr of H_2. Each sample was outgassed under vacuum (10^{-4} Torr). The isotherms were linear in this range. The H_2 chemisorption capacity was calculated by extrapolation of the isotherms to zero pressure.[17]

Pyridine temperature-programmed-desorption (Py-TPD) technique was used to study the acidity of these catalysts. Each catalyst was pretreated in situ in N_2 flow at 350 °C for 1 h. After cooling down to room temperature, the sample was saturated with pyridine, and pure nitrogen was flowed and the temperature increased up to 150 °C until no physically adsorbed pyridine was detected. After baseline stabilization, the temperature was increase at 12 °C min^{-1}, from 150 to 750 °C. Pyridine was detected after methanation using a FID detector.

FTIR spectra of pyridine adsorbed on the samples (Py-IR) were measured to analyze the amount of Brønsted and Lewis acid sites. Spectral measurements were performed on a JASCO FT-IR 5300 spectrometer equipped with a DTGS detector. The range and resolution of acquisition were 4600−400 and 4 cm^{-1}, respectively. A self-supporting wafer for each sample (~20 mg and 13 mm of diameter) was prepared, placed in a thermostated cell with CaF_2 windows connected to a vacuum line, and evacuated for 8 h at 400 °C. The background spectrum was recorded after the sample was cooled to room temperature. Afterward, the solid wafer was exposed to pyridine vapors (Sintorgan, 99% purity) until the system was saturated to 46 Torr at room temperature; the time at this pressure was 12 h. The IR spectrum for each sample was obtained after pyridine desorption by evacuation for 1 h at 250, 350, and 400 °C. All the spectra were recorded at room temperature before and after pyridine adsorption and desorption at each temperature. The difference spectrum was finally obtained by subtracting the background spectrum previously recorded.

The amounts of carbonaceous materials deposited on the spent catalysts were determined by temperature-programmed oxidation (TPO) using a stream of 5% v/v O_2 in N_2 and a heating rate of 12 °C min^{-1}. The oxidation products were detected with a FID detector after methanation.

2.3. Catalytic Activity. The catalytic activity was measured at atmospheric pressure in a continuous-flow fixed-bed reactor. The catalyst was loaded in the reactor using the fraction 40−80 mesh. The catalyst bed was supported with quartz wool, and the reactor was a quartz tube of 5 mm inner diameter. The catalyst was reduced in situ with 30 mL min^{-1} of H_2 (>99.9990%) by heating at 10 °C min^{-1} up to 500 °C and maintaining this value for 1 h, and then decreased to the desired reaction temperature. The carrier gas was saturated by bubbling in liquid anisole maintained at a given temperature to obtain a partial pressure between 3.8 and 15.0 Torr using a flow rate between 5 and 40 mL min^{-1}. To obtain this partial pressure, the temperature of the liquid anisole was adjusted in the range of 25−50 °C. Under these conditions, the space time (W/F) was adjusted between 0.025 and 0.8 g_{cat} h $g_{anisole}^{-1}$. The reactor outlet stream was analyzed online with a GC (SRI 8610) equipped with a ZB-5 capillary column (15 m) and FID detector. A split ratio of 100 was used. Products were identified using standard samples by GC−MS (Varian Saturn 2000) equipped with a HP-5 capillary column. Samples for ex situ analysis were collected in a condenser cooled at 0 °C. At the end of the catalytic test, the catalyst bed was purged with H_2 at the reaction temperature during 30 min. The gas flow rates were controlled with mass flow controllers (Aalborg Instruments and Controls, Inc.).

Product yields and selectivities were calculated using the following concepts:

$$\text{Yield}_i\ (\%) = \text{moles of anisole converted to product } i \times 100/\text{moles of anisole fed}$$

$$\text{Selectivity}_i\ (\%) = \text{moles of anisole converted to product } i \times 100/\text{moles of anisole converted}$$

The activity was measured at different contact times. The W/F was varied between 0.025 and 0.8 g_{cat} h $g_{anisole}^{-1}$ changing the catalyst mass loaded in the reactor and maintaining the hydrogen flow rate and the saturator temperature constant. Values of W/F lower than 0.5 g_{cat} h $g_{anisole}^{-1}$ were obtained by increasing the anisole flow rate and maintaining the catalyst mass constant.

The effect of the reaction temperature was studied with Pt(1.7)/SiO_2 and Pt(1.7)/γ-Al_2O_3 catalysts. The experiments were carried out at W/F = 0.8 g_{cat} h $g_{anisole}^{-1}$, H_2/anisole molar ratio = 83, increasing the temperature in 50 °C steps from 200 to 500 °C, and then the reverse procedure was followed, measuring the activity at the same temperature values. This procedure was adopted to check the catalyst stability by comparison of the activities obtained in the direct and the reverse temperature sequence.

The influence of H_2/anisole molar ratio was also studied with Pt(1.7)/SiO_2 varying the hydrogen partial pressure in the gas flow, fixing the mass of catalyst and W/F (0.19 g_{cat} h $g_{anisole}^{-1}$).

Blank experiments without catalysts were carried out to determine the contribution of the thermal conversion. The activity of the pure supports was also evaluated.

2.4. Catalyst Regeneration. Catalyst regeneration was carried out after reactions at W/F = 0.08 g_{cat} h $g_{anisole}^{-1}$ and 300 °C with Pt/γ-Al_2O_3, at W/F = 0.02 g_{cat} h $g_{anisole}^{-1}$ and 300 °C with Pt/SiO_2 and W/F = 0.05 g_{cat} h $g_{anisole}^{-1}$ and 400 °C with Pt/Na−B catalysts. The conditions were chosen to observe deactivation and therefore to evaluate the effectiveness of the regeneration procedure. After 3 h of reaction, the catalysts were purged for 30 min in H_2 and then 30 min in N_2. Afterward, the catalysts were treated 1 h in air at 350 °C, activated 1 h in H_2, and a new reaction cycle was carried out. Another regeneration treatment was also carried out by treating the catalyst in H_2 at 500 °C instead of using air at 350 °C.

2.5. Carbon Balance. Carbon balances after the catalytic tests were calculated as in a previous article.[6] As the light hydrocarbons were not analyzed in detailed in all samples, the carbon balance was carried out in an extreme situation, assuming that light hydrocarbons are mostly methane. The average values of product yields and reactant conversion during the reaction were considered for the calculations. Carbon deposited on the catalyst determined by TPO analysis was taken into account.

3. RESULTS AND DISCUSSION

3.1. Catalyst Characterization. The catalysts used in this work have been previously studied in the hydrodeoxygenation of m-cresol.[7] To facilitate the discussion, the main characterization results are summarized in this section. The Pt(1.7)/γ-Al_2O_3 is a typical mesoporous catalyst with a surface area of 214 m^2 g^{-1}. The Pt(1.7)/SiO_2 catalyst had a total surface area of

DOI: 10.1021/acs.iecr.7b00521
Ind. Eng. Chem. Res. 2017, 56, 6419−6431

359 m^2 g^{-1}, with 57 m^2 g^{-1} of micropores and 302 m^2 g^{-1} of mesopores. The total surface area of Pt(1.7)/Na−B resulted to be 506 m^2 g^{-1}, with 303 m^2 g^{-1} of micropores and 203 m^2 g^{-1} of mesopores, and similar results were found for the Pt(1.7)/NaH-B catalyst. The adsorption−desorption isotherm for the pattern HBEA and the Na−B catalysts were approximately the same and showed a nonpronounced hysteresis loop, which indicated that the relatively high value of mesoporous area corresponded to external surface area contributions rather than to intracrystalline porosity. The micropore volume was 0.19 cm^3 g^{-1}, which is a typical value for the BEA framework.[18] These results are presented in Table S1 (Supporting Information).

As mentioned in the experimental part (section 2.1) the Pt(1.7)/Na−B catalyst contains 1 wt % sodium. According to the International Zeolite Association, a Beta zeolite with Si/Al = 13 has the formula $Na_{4.53}$ $[Al_{4.53}Si_{59.47}O_{128}]$. Therefore, the sodium content of this material is 2.2 wt %. This means that in the support used in this study the sodium content is approximately 50% of the maximum theoretical value. The other fraction of sites is in the protonic form.

The X-ray diffractogram of the Pt(1.7)/γ-Al_2O_3 catalyst displayed signals at 2θ = 45.901, 67.093, 37.635, 39.524, and 19.466, which correspond to the alumina support (JCPDS-ICDD 10−425). There were no signals in the diffractogram that corresponded to Pt (JCPDS-ICDD 4−802), which indicated that the particles were small and consequently, the metal had a high dispersion. In the diffractogram of Pt(1.7)/SiO_2 catalyst, only an amorphous halo with a characteristic peak at 2θ = 23.8° was observed.

The diffractogram of the Pt(1.7)/Na−B catalyst showed that there were no significant changes in the zeolitic structure due to the ion exchange treatment in sodium hydroxide. The crystallinity degree of this catalyst was 90%, taking 100% for the original H−B zeolite. Figure S1 (Supporting Information) shows the XRD patterns of the zeolite-based catalysts.

The average particle sizes of Pt were 1.5 and 1.9 nm for the Pt(1.7)/γ-Al_2O_3 and Pt(1.7)/SiO_2 catalysts, respectively, as determined by TEM. As expected, smaller Pt particles are present on alumina compared to the silica support. This means that in these catalysts, the Pt particles can easily be accommodated in the pores of the support. Figure S2 (Supporting Information) shows the images obtained by TEM of these two catalysts. It can be clearly observed the small Pt particles in both supports. The metallic dispersions calculated by H_2 chemisorption for all the catalysts tested are shown in Table 1. It can be observed that the dispersion values obtained with this technique were very similar for all of the catalysts. On one hand, there is no direct correlation with the results obtained using TEM, although there is not a major difference. On the other hand, since the Pt particles are similar in size in all the catalysts, it can be expected that the metal function is not the reason for the catalytic differences observed among these catalysts, being this a key issue to understand the bifunctional reaction mechanism involved in the anisole deoxygenation.

Table 1. Metal Dispersion (Hydrogen Quimisorption), Acid Sites Densities (Py-TPD), and TOF

catalyst	metal dispersion (%)	total acid sites density (μmol Py/m^2 cat.)	TOF[a] (s^{-1}) metal[b]	TOF[a] (s^{-1}) acid[c]
Pt/SiO_2	25	0.023	1.2	2.630
Pt/γ-Al_2O_3	22	0.279	1.3	0.400
Pt/Na−B	21	2.360	1.3	0.019
Pt/NaH-B	20	5.150	1.2	0.009

[a]Average TOF, reaction conditions: see legend to Figures 3. [b]Molecule of anisol converted/(atom of exposed Pt s). [c]Molecule of anisol converted/(acid site s).

The TPR profile of the Pt(1.7)/γ-Al_2O_3 catalyst displayed one peak at 240 °C and a second one at 414 °C. It has been reasonably established that the first peak corresponds to the bulk phase of the PtO_x and the second reduction peak to highly dispersed particles with strong interaction with the support.[19−21] In the case of the Pt(1.7)/SiO_2 catalyst, there were also two peaks, but at lower temperatures, being the first one at 127 °C and the second one at 300 °C. The TPR profile of Pt/Na−B catalyst had the two peaks at 100 and 485 °C. According to these results, all the catalysts were reduced before the reaction at 500 °C for 1 h.

The total acid sites densities obtained by Py-TPD experiments are shown in Table 1. It can be observed that it increases in the order: Pt(1.7)/SiO_2 ≪ Pt(1.7)/γ-Al_2O_3 ≪ Pt(1.7)/Na−B < Pt(1.7)/NaH-B. The profiles deconvolution identifies three different desorption maxima peaks of pyridine at low-temperature, medium-temperature, and high-temperature regions, thus suggesting the presence of weak, medium, and strong acid sites, respectively. As shown in Figure 1, the

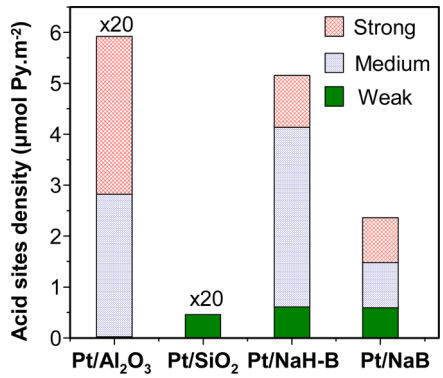

Figure 1. Total density and acid sites distribution obtained by pyridine TPD.

Pt(1.7)/γ-Al_2O_3 catalyst has mostly strong and medium strength acid sites, and the Pt(1.7)/SiO_2 has only weak acid sides. On the other hand, the zeolites materials have a broader acid strength distribution. It is interesting to observe that the total number of acid sites present in the Pt(1.7)/Na−B catalyst is approximately half of that obtained in the Pt(1.7)/NaH-B catalyst, in agreement with the Na content analysis, which indicated that practically half of the sites are in the protonic form. The nature of the acid sites present in each catalyst was analyzed by FTIR spectroscopy after pyridine adsorption. Results are shown in Figure 2. The Pt(1.7)/SiO_2 did not show any signals. This means that the acid sites present in this catalyst are so weak that the pyridine desorbs during the evacuation at 250 °C in vacuum before the IR measurement, or in the case of the Brønsted acid sites are very weak and cannot protonate the pyridine molecule to the corresponding pyridonium ion. The Pt(1.7)/γ-Al_2O_3 catalyst presents only signals corresponding to Lewis acidity, at 1622, 1580, 1470, and

DOI: 10.1021/acs.iecr.7b00521
Ind. Eng. Chem. Res. 2017, 56, 6419−6431

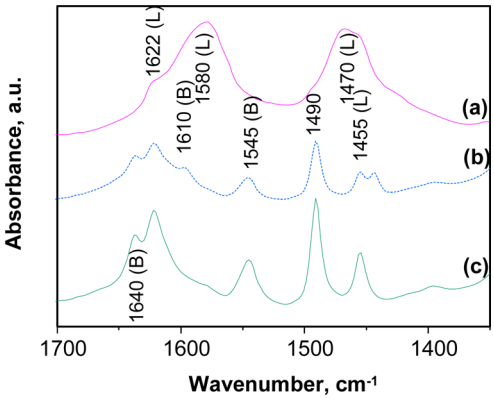

Figure 2. FTIR spectrum of the catalysts after pyridine adsorption and desorption at 250 °C: (a) Pt(1.7)/γ-Al_2O_3, (b) Pt(1.7)/Na−B, (c) Pt(1.7)/NaH-B.

1455 cm^{-1}, and the Pt(1.7)/Na−B and Pt(1.7)/NaH-B catalysts present both, Lewis and Brønsted acidity, with signals at 1455 and 1545 cm^{-1}, respectively. Quantitative results for the Pt/zeolites catalysts are shown in Table 2. The acidity of Pt(1.7)/Na−B is lower than the acidity of Pt(1.7)/NaH-B, as expected.

Table 2. Acid Sites Concentration Obtained by Py-FTIR[a]

catalyst	Br sites (mmol g^{-1})	Le sites (mmol g^{-1})	Br + Le (mmol g^{-1})
Pt/Na−B	0.24	0.13	0.37
Pt/NaH-B	0.52	0.30	0.82

[a]Brønsted and Lewis concentrations determined by the 1545 and 1455 cm^{-1} signals, respectively.

3.2. Catalytic Activity. A blank experiment without catalyst, in H_2 flow (5 mL min^{-1}) at 500 °C, was carried out to determine the conversion due to the thermal decomposition. Only anisole was observed at the reactor outlet.

3.2.1. Catalytic Activity of the Supports. The activity of pure alumina was evaluated at W/F = 0.1 g_{cat} h $g_{anisole}^{-1}$ and 400 °C by obtaining an anisole conversion of 92% at 20 min of reaction, the main products being phenol (40.2%), cresol (43.4%), and other heavier oxygenated compounds (7.9%). Only 0.28% was transformed into light products. At 160 min of reaction, the conversion dropped to 66%, with 100% of selectivity to oxygenates, with phenol yield of 24%, 37% of cresol, and 3.8% of heavier oxygenates. The amount of coke formed on this support was 19.4%, which is a very high value (see Table 3).

An additional experiment was performed using pure silica as catalyst under the same conditions. Conversion of anisole was zero from the beginning of the reaction, and the amount of coke deposited was 1.2%.

3.2.2. Catalytic Activity of Pt(1.7)/SiO_2 in the Anisole Deoxygenation Reaction. The Pt(1.7)/SiO_2 catalyst can be considered as a metallic catalyst, since the SiO_2 support has a very low acidity, as seen in Table 1. The conversion and yields obtained during the reaction at 400 °C, W/F = 0.1 g_{cat} h $g_{anisole}^{-1}$, and H_2/anisole ratio = 83 are shown in Figure 3. The main reaction products were phenol, benzene, and light products (LH) composed mainly of methane. Phenol is obtained by anisole demethylation, while benzene is formed by phenol deoxygenation. Since this support has almost no

Table 3. Coke Deposits on Spent Catalysts

catalyst	space time (W/F) g_{cat} h $g_{anisole}^{-1}$	H_2/anisole molar ratio	$T_{reaction}$ (°C)	coke %
Pt/SiO_2	0.025	83	400	6.54
Pt/SiO_2	0.05	83	400	4.33
Pt/SiO_2	0.10	83	400	2.21
Pt/SiO_2	0.50	83	400	1.05
Pt/Al_2O_3	0.10	83	400	9.14
Pt/Na−B	0.10	83	400	9.44
Pt/NaH-B	0.10	83	400	9.21
Pt/SiO_2	0.31	40	300	1.21
Pt/SiO_2	0.19	40	300	1.37
Pt/SiO_2	0.19	201	300	1.24
Pt/SiO_2	0.19	730	300	1.02
Al_2O_3	0.10	83	400	19.40
SiO_2	0.1	83	400	1.20

acidity, it is evident that the demethylation occurs via a metal-catalyzed step as well as the phenol deoxygenation, as also suggested by M. A. González-Borja and D. E. Resasco.[8] In a previews work, we studied the deoxygenation of cresol (methylphenol) and phenol to toluene and benzene, respectively.[5] It has been proposed that the deoxygenation reaction occurs on the metal after the aromatic ring is partially hydrogenated, and then the C−OH bond breakage occurs by acid catalyzed dehydration, followed by dehydrogenation of the ring.[22] Additionally, a low amount of Ar-OR products was found, as shown in Figure 3, including methyl anisoles and methyl phenols. These oxygenated products are formed on the acid sites, which are mostly Brønsted sites in this case, being this type of acid sites needed to catalyze these reactions.[22] The GC−MS analyses of the collected products indicated the presence of "others" products, formed by condensation reactions, like biphenyl, dimethyl-diphenyl, 1-methoxy-4-(phenylmethyl) benzene, and 2,2′-benzophenone.

The different reactions that take place in this system are shown in Scheme 1, including deoxygenation and condensation reactions,[5,6] and mono and bimolecular transalkylations (isomerization and disproportionation) as observed by other authors.[4,8,15,23] Each of these reactions occurs by a mechanism that may involve several steps, each of which takes place on a particular type of site. In each reaction, it is indicated if an acid (A) or a metal (M) site is involved in the reaction mechanisms. The $-CH_3$ fragments alkylate oxygenated aromatics that form part of the pool of Ar-OR products, and therefore, the yield of lights compounds (mainly methane) does not increase as phenol yield does, reaching a steady-state. Besides the formation of phenol by anisole demethylation, a small fraction of phenol is formed on the acid sites by disproportionation, as shown in the reaction network of Scheme 1. Then it can be inferred that as the acid function is deactivated, the amount of phenol obtained by disproportionation also decreased. The results shown in Figure 3 suggest that on Pt(1.7)/SiO_2 the main reaction path is anisole → phenol → benzene on the metal sites. The very low acidity of this catalyst is not enough to catalyze the other reaction paths shown in the reaction network of Scheme 1. In the first step, the energy required to break the ArO−CH_3 bond is approximately 385 kJ/mol, while the direct demethoxilation, that is, to break the Ar-OCH_3 bond, requires 422 kJ/mol.[13] It is important to highlight that the Ar−OH bond is even higher, approximately 468 kJ/mol, and because of this, it is not possible to directly break this bond, and a previous

DOI: 10.1021/acs.iecr.7b00521
Ind. Eng. Chem. Res. 2017, 56, 6419−6431

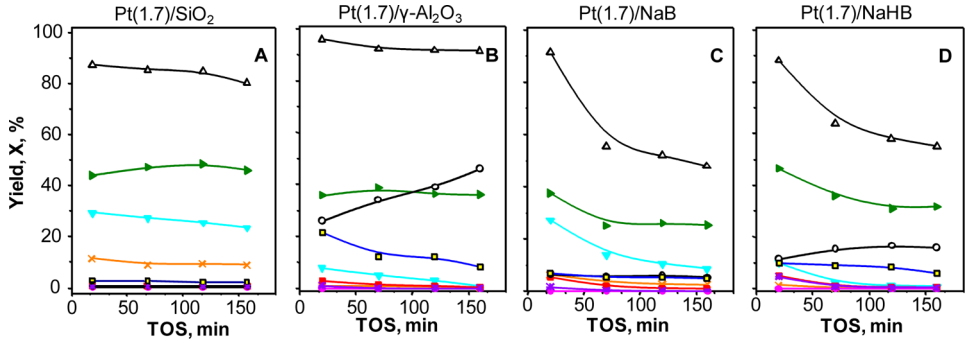

Figure 3. Anisole conversion and product yields versus time on stream at 400 °C, H_2/anisole molar ratio = 83, W/F = 0.1 g_{cat} h $g_{anisole}^{-1}$ for: (A) Pt(1.7)/SiO_2; (B) Pt(1.7)/γ-Al_2O_3; (C) Pt(1.7)/Na–B; (D) Pt(1.7)/NaH-B. References: (open delta) anisol conversion, (orange) light products, (cyan) benzene, (magenta) methylcyclohexane, (red) toluene, (violet) xylenes, (green) phenol, (open circle) Ar-OR, (open square) others.

Scheme 1. Proposed Reaction Network for Anisole Deoxygenation over Pt/γAl_2O_3

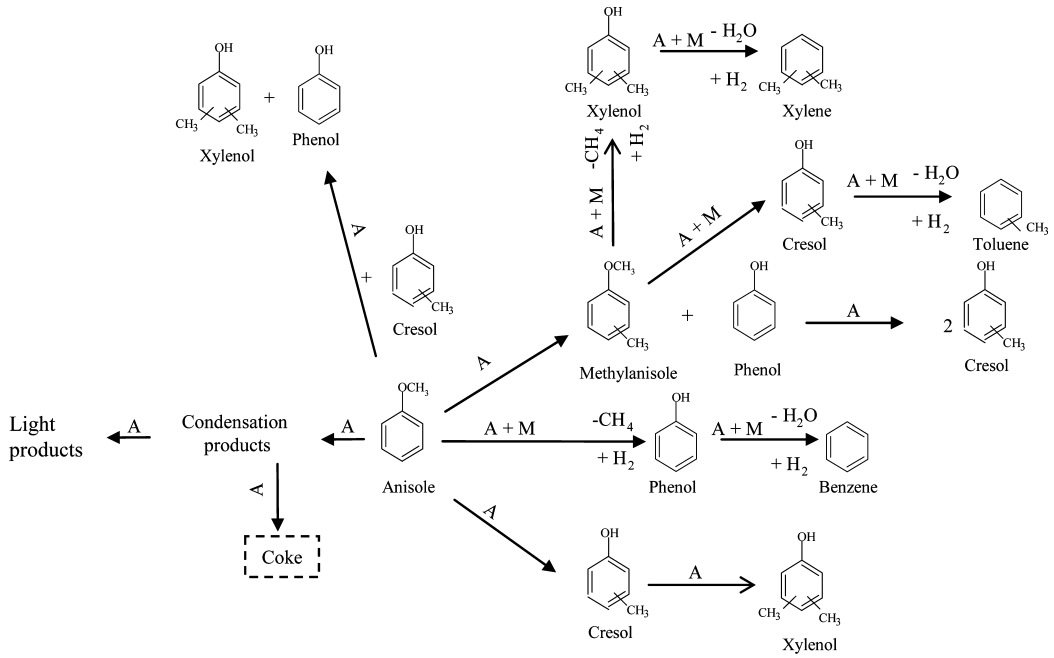

partial hydrogenation of the aromatic ring is needed, followed by a dehydration step, which is easily catalyzed by acid sites.[22] In the nonacidic supports, such as the Pt(1.7)/SiO_2 used in this study, the direct deoxygenation on the metal occurs, probably via a mechanism involving a fast enol-keto tautomerization of the phenol before the ring hydrogenation, forming an unsaturated alcohol that is readily dehydrated.[24,25]

The evolution of conversion and products yields as a function of space time (W/F), at 400 °C, and H_2/anisole ratio = 83, for the Pt/SiO_2 catalyst is shown in Figure 4. As space time increased, benzene selectivity also increased. For the highest space time, it was observed that demethylation plus deoxygenation were the dominant reactions and the acid catalyzed transalkylation reactions less important. On the other hand, as space time decreased, more products were obtained via acid-catalyzed reactions (methyl anisoles, methyl phenols), which indicated that these compounds are primary products as it is shown in Scheme 1.

Figure 5 shows the TPO profiles, and Table 3 shows the amount of coke formed on the catalysts at different reaction conditions. It can be observed that the amount of coke deposited on the Pt/SiO_2 catalyst decreases as the space time increases. This suggests that the main precursor for coke formation is the reactant, and therefore, it has been included in the reaction network presented in Scheme 1. Similar results were obtained when using m-cresol as feed with lower amount of coke formed at higher space times, therefore forming a decreasing coke profile along the catalyst bed[7] that corresponds to the parallel coke formation mechanism, in which coke is formed mainly from the reactant. Besides, Figure 5 shows that the relationship between the cokes deposited on the metal sites (first peak in the TPO profile), and the corresponding to the acid sites (second peak) increases as the space time decreases. Therefore, this difference in coke deposition on the metal and on the acid sites is also a cause of change in selectivity as the catalyst deactivates.

The balance of C was performed for Pt/SiO_2 catalyst after a reaction of 160 min at 400 °C, W/F = 0.02 h, H_2/anisole = 83. Carbon recovery was 83%, assuming that the light hydrocarbons are mostly methane, and 92% considering an average amount of 4 C per molecule of the light fraction.

3.2.3. Catalytic Activity of Pt(1.7)/γ-Al_2O_3 in the Anisole Deoxygenation Reaction. Pt(1.7)/γ-Al_2O_3 catalyst was also tested for the anisole deoxygenation at 400 °C. Figure 3B

DOI: 10.1021/acs.iecr.7b00521
Ind. Eng. Chem. Res. 2017, 56, 6419–6431

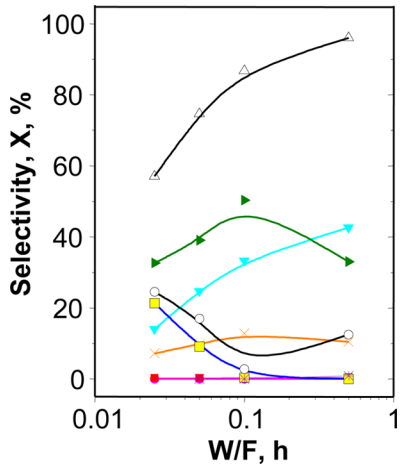

Figure 4. Anisole conversion and product selectivity versus space time (W/F) for Pt(1.7)/SiO_2 after 20 min of reaction at 400 °C, H_2/anisole molar ratio = 83. References: (open delta) anisol conversion, (orange) light products, (cyan) benzene, (magenta) methylcyclohexane, (red) toluene, (violet) xylenes, (green) phenol, (open circle) Ar-OR, (open square) others.

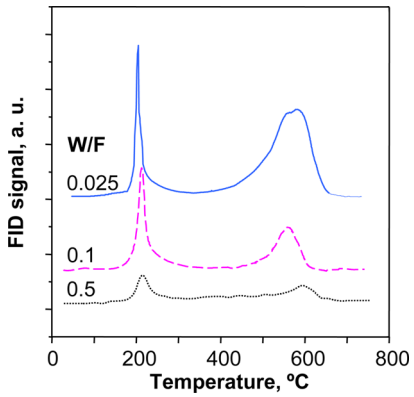

Figure 5. TPO profiles and the amounts of coke burnt for the different space times, after 136 min of reaction at 400 °C, H_2/anisole molar ratio = 83. Catalyst: Pt(1.7)/SiO_2. References: W/F, g_{cat} h $g_{anisole}^{-1}$.

shows the anisole conversion and product yields versus time on stream. The Pt(1.7)/γ-Al_2O_3 catalyst is much more selective to oxygenated products (Ar-OR) than Pt(1.7)/SiO_2 catalyst (Figure 3A), compared at similar conversion levels. These products are formed by condensation and transalkylation reactions as described for the Pt(1.7)/SiO_2 catalyst, being the phenol and methylanisol formed by anisole disproportionation. Cresol is formed by anisole isomerization and forms toluene by a subsequent deoxygenation. All these reactions are shown in Scheme 1. However, during the m-cresol deoxygenation with Pt(1.7)/γ-Al_2O_3 and Pt(1.7)/SiO_2, it was observed that the initial selectivity to deoxygenated products (toluene) was the same for both catalysts.[7] This was because the hydrodeoxygenation of m-cresol to toluene was the fastest reaction when the Pt content was high enough, for example, 1.7 wt %. On the other hand, during the anisole deoxygenation on Pt(1.7)/γ-Al_2O_3 (through demethylation follow by phenol deoxygenation), the acid-catalyzed reactions play a more significant role than during the cresol deoxygenation, and therefore, the different catalytic behavior of these two catalysts is caused by the differences in the metallic/acid sites ratio and in the acid strength of the two supports. In summary, the higher selectivity to oxygenated compounds (Ar-OR) obtained with Pt(1.7)/γ-Al_2O_3 compared to Pt(1.7)/SiO_2 is due to the higher acidity of the alumina compared to the silica, as shown in Figure 1. Therefore, there are several oxygenated primary products that are obtained with the Pt(1.7)/γ-Al_2O_3 catalyst. The acidity of the alumina corresponds to Lewis acid sites, although it also contains Brønsted sites due to the presence of acidic hydroxyl groups.[25] These Brønsted sites are weak and cannot protonate pyridine,[26] and for this reason, these sites are not observed in the FTIR of adsorbed pyridine. However, these sites can catalyze the dehydration reaction.[27] It is important also to observe the difference in the selectivity to light products between Pt(1.7)/γ-Al_2O_3 and Pt(1.7)/SiO_2, having the former a much lower yield to these products, due to the higher activity for alkylating the aromatic ring with the $-CH_3$ fragments. Because of this, the Pt(1.7)/γ-Al_2O_3 has higher production of Ar-OR compounds and lower selectivity to light products than the Pt(1.7)/SiO_2 catalyst.

As a result of carbon balance calculation, after a reaction of 160 min at 400 °C, W/F = 0.08 h, H_2/anisole = 83 with the Pt(1.7)/Al_2O_3 catalyst, and carbon recovery assuming that light hydrocarbons were mostly methane was 99.2%. However, as mentioned above, there are other compounds with greater amount of C; therefore, the loss may be less than 0.8%. Additionally, for 160 min at 400 °C, W/F = 1.3 h, H_2/anisole = 131, and recovery of C was 99.9%.

3.2.4. Catalytic Activity of Pt(1.7)/Na−B and Pt(1.7)/NaH-B in the Anisole Deoxygenation Reaction. The Pt(1.7)/Na−B catalyst (Figure 3C), despite having higher total acid site density, is more selective to benzene than Pt(1.7)/γ-Al_2O_3 (Figure 3B). There are other important differences in selectivity between these two catalysts. Pt(1.7)/Na−B generates a higher amount of light products and much lower amount of Ar-OR compounds. All these results were obtained at 400 °C.

By comparing Pt(1.7)/Na−B (Figure 3C) with Pt(1.7)/SiO_2 (Figure 3A) catalysts, it can be observed that there are no significant differences in product selectivities, except that Pt(1.7)/Na−B catalyst is more selective to the Ar-OR products formed by acid catalyzed anisole transalkylation reactions. Also, lower amounts of light products were obtained with the Pt(1.7)/Na−B catalyst. The products called "Ar-OR", as mentioned before, are formed on the acid sites. Part of the $-CH_3$ fragments obtained in the anisole demethylation reaction participates in acid catalyzed alkylation reactions producing methyl phenols and methyl anisoles. Because of this, the yield of light products is lower on Pt(1.7)/Na−B than in Pt(1.7)/SiO_2 catalyst. The higher acidity of the Pt(1.7)/Na−B catalyst explains these results.

To study the effect of the acidity on the anisole deoxygenation reaction, the Na−B support was exchanged with ammonium to generate higher acidity, maintaining the pore structure. This catalyst was called Pt(1.7)/NaH-B. As observed in Table 2, the acid sites density for Pt(1.7)/NaH-B is significantly higher than that in the Pt(1.7)/Na−B catalyst.

Figure 3C and D allow the comparison in product distribution at the same initial conversion level. With the Pt(1.7)/Na−B catalyst, demethylation and deoxygenation are the main reactions. The yields of Ar-OR are higher for Pt(1.7)/NaH-B catalyst due to the higher acid density that facilitate bimolecular reactions such as transalkylation. However, the yield of light products is lower since the acidity promotes the alkylation of other molecules with the $-CH_3$ fragments, avoiding carbon loss. Then an intermediate level of acidity is

DOI: 10.1021/acs.iecr.7b00521
Ind. Eng. Chem. Res. 2017, 56, 6419−6431

needed to obtain a balance between a maximum of deoxygenated products and a minimum carbon loss. Bifunctional catalysts exhibit a unique advantage for the deoxygenation conversion of aromatic compounds containing a methoxy group in comparison with any other catalysts where carbon loss is unavoidable. In the hydrocracking process at low temperature carried out on acid catalysts containing no metals, the methoxy group is removed as methanol. Furthermore, in hydrotreating processes at high temperature using sulfided catalysts, there is a great carbon loss as methane.[5] In Pt/beta-zeolite, most methyls groups are transferred to the aromatic ring and retained after deoxygenation minimizing carbon loss.

The beta zeolite is a typical microporous material, and taking into account the high conversions obtained with the Pt(1.7)/Na−B and Pt(1.7)/NaH-B catalysts, it is very likely that the reaction proceeds in the presence of internal mass transfer limitations. The Weisz-Prater criterion establishes that if the parameter C_{wp} defined in eq 1 is higher than 0.3, there is internal mass transfer limitation:

$$C_{wp} = (-r_a \rho R^2)/(De C_a) \quad (1)$$

where $(-r_a)$ is the rate of anisol consumption, ρ is the beta-zeolite density, R is the crystal radius, De is the effective diffusivity of anisole, and C_a is its concentration in the crystal surface. The average reaction rate throughout the reactor was 76 mmol g^{-1} h^{-1} (see TOF values in Table 1) calculated using the first conversion value shown in Figure 3. The Knudsen diffusivity at 673 K for anisole is 1.7 10 $^{-3}$ cm^2 s^{-1}. The concentration of anisole in the gas phase is 2.2×10^{-4} mol L^{-1}. There are uncertainties in the tortuosity factor and in the crystal size. By using a typical value of 0.4 μm for the crystal size, the C_{wp} results to be higher than 10. This value clearly indicates that the reaction proceeds with internal mass transfer limitations in the beta zeolite supported catalysts. This phenomenon obviously masks the intrinsic activity of these catalysts and modifies the product distribution compared to the mesoporous catalysts.

The fast deactivation of the zeolite catalysts (Figure 3C,D) is attributed to the high amount of carbon deposits formed in these catalysts, as shown in Table 3, which certainly is related to the higher acidity and microporous structure. Pore blocking is a reason for a rapid decrease in conversion. The formation of coke on Pt/γ-Al_2O_3 also was high. In Figure 3B, substantial changes are observed in the distribution of products with reaction time, but the conversion was maintained in high values. Nevertheless, even with a similar level of coke on Pt(1.7)/γ-Al_2O_3, Pt(1.7)/Na−B, and Pt(1.7)/NaH-B, the effect on the activity is more important in the two catalysts supported on Beta zeolite. This is because in the microporous catalysts, the pore blocking leads to a faster loss of active sites than in the case of a mesoporous support, such as alumina. In addition, the coke deposition in the zeolite channels strongly increases the diffusional limitations in these catalysts, even when no pore-mouth plugging occurs.

Carbon balance after a reaction of 160 min at 400 °C, W/F = 0.02 h, H_2/anisole = 83 was calculated for Pt/NaB catalyst. Carbon recovery was 80% considering light products are methane and 90% assuming an average amount of 4 C per light molecule.

3.2.5. Effect of Acidity on Catalytic Performance. Figure 6 shows the yields at 20 min of reaction obtained in experiments carried out at W/F = 0.1 g_{cat} h $g_{anisole}^{-1}$, H_2/anisole molar ratio of 83, and a temperature of 400 °C, as a function of the total acid sites density of the catalysts used in each experiment (shown in Table 1). The relationship between yields and acid sites density is quite complex, and it seems to be strongly dependent on the type of porous structure. For example, the production of benzene is practically the same on Pt/SiO_2 as on Pt/NaB, while the acid sites density is 100-times higher in the second catalyst. In each group of mesoporous and microporous catalysts, the production of deoxygenated compounds decreases as the acid sites density increases. Also, the yield of benzene is similar in Pt(1.7)/γ-Al_2O_3 and Pt(1.7)/NaH-B, while the total acid sites density is approximately 20-times higher in the latter. The silica supported catalyst has higher production of benzene than the alumina supported one, but it displays an important carbon loss as indicated by the formation of higher amounts of the light fraction, due to the lower alkylating activity of the silica support. As above-discussed, the Pt(1.7)/NaH-B catalysts operate under internal mass transfer limitation, and this leads to the discontinuity in the relationship between yields and acid sites density shown in Figure 6.

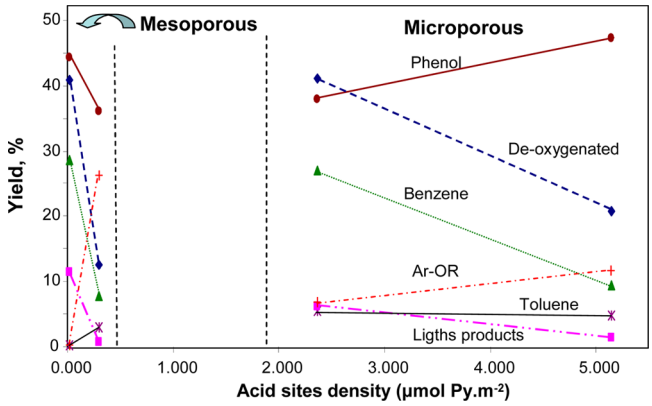

Figure 6. Product distribution obtained at 400 °C, H_2/anisole molar ratio = 83, W/F = 0.1 g_{cat} h $g_{anisole}^{-1}$, as a function of the acid sites density.

Table 1 shows the TOF values, calculated as an average value between the inlet and the outlet of the reactor at 20 min time-on-stream. Taking into account the complexity of the reacting system and the uncertainty regarding which are the reaction rate controlling sites, the TOF values have been calculated both referred to the exposed metal sites and to the number of acid sites. It can be observed that the TOF values based on the available Pt atoms are practically the same for all the catalysts, while the TOF calculated based on the acid sites changes in more than three orders of magnitude between the Pt/SiO_2 and the Pt/NaH-B. Taking into account that the latter has acid sites with a wide distribution of strength, while the former has only weak acid sites in low amounts, the results suggest that the metal function is controlling the anisole conversion, and the support modifies the product distribution and the stability. It has to be kept in mind that there are mass transfer limitations in the microporous catalysts, and therefore, the TOF values do not strictly represent the intrinsic kinetics of this system.

3.3. Effect of Reaction Temperature. Reactions at 300 and 400 °C were carried out with Pt/SiO_2 catalyst, at W/F = 0.19 g_{cat} h $g_{anisole}^{-1}$, H_2/anisole = 40, during 160 min. After the reaction, the carbon deposits were quantified by TPO. The spent catalysts presented 1.37 and 7.23% of carbon after reaction at 300 and 400 °C, respectively. There is a strong

DOI: 10.1021/acs.iecr.7b00521
Ind. Eng. Chem. Res. 2017, 56, 6419−6431

influence of the reaction temperature on the amount of coke deposited on the catalyst.

The influence of the reaction temperature on product selectivity was also evaluated with the Pt/SiO_2 catalyst. The conversion and products yields as a function of reaction temperature are shown in Figure 7, both as the temperature was

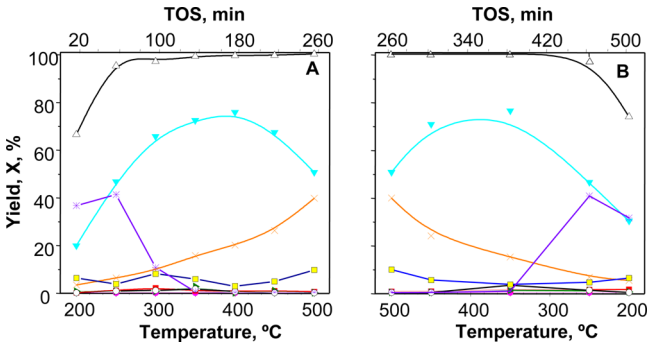

Figure 7. Anisole conversion and product yield versus temperature. Catalyst: $Pt(1.7)/SiO_2$, H_2/anisole molar ratio = 83, W/F = 0.8 g_{cat} h $g_{anisole}^{-1}$, (A) Increasing temperature from 200 to 500 °C. (B) Decreasing temperature from 500 to 200 °C References: (open delta) anisole conversion, (orange) LH, (cyan) benzene, (magenta) methylcyclohexane, (red) toluene, (violet) xylenes, (green) phenol, (open circle) Ar-OR, (open square) others.

increased and as it was decreased (Figure 7A and B, respectively). The space time for this reaction was 0.8 g_{cat} h $g_{anisole}^{-1}$ and the H_2/anisole molar ratio 83.

The results obtained in both paths are very similar and indicate that there was no significant deactivation during this experiment. Therefore, the tendency observed is qualitatively representative of the catalytic behavior at each temperature at initial reaction time. It is possible to obtain deoxygenated products throughout all the temperature range studied. Furthermore, light products are obtained by either demethylation or cracking reactions with higher yields at higher temperatures, as also observed during cresol deoxygenation reactions.[5] Xylenes are only observed at temperatures below 400 °C. Under the conditions used, with a high W/F, the phenol was completely transformed in benzene, and therefore, it was not obtained as a reaction product.

The sum of benzene (RON = 101) and xylene (RON = 118) yields has a maximum at 250 °C. Besides, at this temperature, the ratio (benzene + xylene)/(light products + oxygenates) is the highest. Thus, 250 °C is the optimal temperature at this space time for anisole deoxygenation on Pt/SiO_2.

Compared with results shown in Figure 3A, which were obtained with a W/F = 0.1 g_{cat} h $g_{anisole}^{-1}$, it can be observed that at 400 °C, there is a much higher amount of lights compounds at the higher space time (Figure 7), and in this condition, there are not Ar-OR compounds, which indicates that the latter are clearly intermediates in the reaction network shown in Scheme 1.

The influence of temperature on the reaction product distribution was also evaluated using the $Pt/\gamma\text{-}Al_2O_3$ catalyst. Conversion rates and yields as a function of the reaction temperature are shown in Figure 8. The space time for this reaction was 0.8 g_{cat} h $g_{anisole}^{-1}$ and the H_2/anisole molar ratio 83. In this case, it was also possible to obtain deoxygenated products throughout the temperature range studied. Light compounds production was favored at higher temperatures.

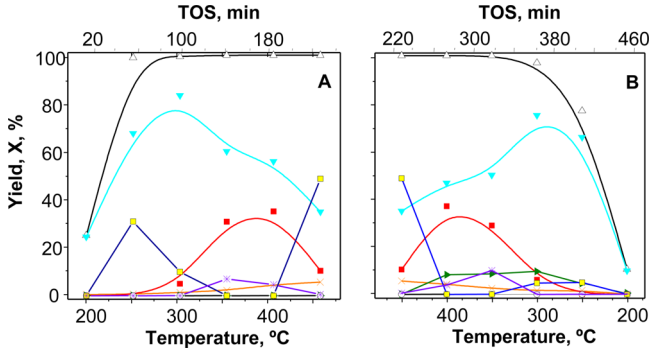

Figure 8. Anisole conversion and product yield versus temperature. Catalyst: $Pt(1.7)/\gamma\text{-}Al_2O_3$. H_2/anisole molar ratio = 83, W/F = 0.8 g_{cat} h $g_{anisole}^{-1}$. (A) Increasing temperature from 200 to 500 °C. (B) Decreasing temperature from 500 to 200 °C. References: (open delta) anisole conversion, (orange) LH, (cyan) benzene, (magenta) methylcyclohexane, (red) toluene, (violet) xylenes, (green) phenol, (open circle) Ar-OR, (open square) others.

Xylenes were only observed between 300 and 450 °C, with a maximum at 350 °C, showing a different behavior than Pt/SiO_2. Toluene maximum production was obtained between 350 and 400 °C, while the benzene selectivity decreased as a function of the temperature. This experiment was carried out with a high space time, and because of this, phenol formed was completely deoxygenated to benzene during the temperature ascending path. Because of deactivation, phenol was observed in the temperature descending path. A very important result shown in Figure 8 is that at 200 °C, the deoxygenation of anisole proceeds with a very high selectivity to benzene, although with a low conversion.

The sum of the yields of benzene, xylene, and toluene is maximized at 300 °C. At this temperature, the ratio of (benzene + toluene + xylene)/(light products + oxygenates) is maximized. Therefore, 300 °C is the optimum temperature for anisole deoxygenation with $Pt/\gamma\text{-}Al_2O_3$, with a very high selectivity to deoxygenated products and a high activity.

The important conclusion is that regardless the space time used in these reactions, there is an optimal intermediate temperature to obtain deoxygenated products without a significant carbon loss and deactivation by carbon deposits.

3.4. Effect of H_2/Anisole Ratio. The effect of the H_2/anisole molar ratio was evaluated with the Pt/SiO_2 catalyst at 300 °C, since at higher temperatures low yields of deoxygenated products were observed, without obtaining xylenes as shown in the previous section. The ratio was varied by changing the partial pressure of H_2 in a stream of N_2 by keeping the total flow rate of 40 mL min^{-1}. The products distribution obtained at W/F = 0.19 g_{cat} h $g_{anisole}^{-1}$ and H_2/anisole ratios of 40 and 201, are shown in Figure 9A and B, respectively.

Under these conditions, the amounts of coke deposited on the Pt/SiO_2 catalyst were 1.37 and 1.24 wt %, respectively (Table 3), which indicated that the hydrogen partial pressure slightly modified the coke deposition. However, the conversion level was approximately 20% higher at the higher H_2/anisole ratio, being the production of xylenes and benzene the main difference.

To elucidate whether the presence of xylenes is related to the higher conversion or to an effect of the H_2/anisole ratio, a new reaction was carried out to have the same conversion level as that shown in Figure 9B, approximately X = 75−80%, by

DOI: 10.1021/acs.iecr.7b00521
Ind. Eng. Chem. Res. 2017, 56, 6419−6431

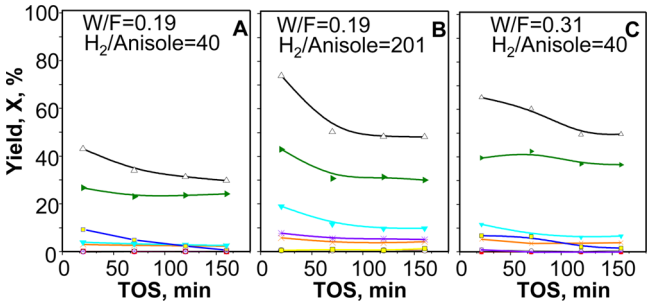

Figure 9. Anisole conversion and product yields versus time on stream for Pt(1.7)/SiO_2 at 300 °C. (A) W/F = 0.19, H_2/anisole = 40; (B) W/F = 0.19, H_2/anisole = 201 (C) W/F = 0.31, H_2/anisole = 40. References: (open delta) anisole conversion, (orange) LH, (cyan) benzene, (magenta) methylcyclohexane, (red) toluene, (violet) xylenes, (green) phenol, (open circle) Ar-OR, (open square) others.

changing the space time but using a H_2/anisole ratio = 40 (Figure 9C). Xylenes were practically not observed and the benzene yield was lower in this case. Therefore, the differences between Figure 9A and B is not only due to the difference in conversion. The H_2/anisole molar ratio plays an important role in the relative rates of the reactions involved in the system. However, since both the xylenes and benzene are products obtained after a sequence of reactions, it is expected that these products do not appear at low conversions. In agreement with this comment, results shown in Figure 7, obtained at a higher W/F (0.80 g_{cat} h $g_{anisole}^{-1}$), show that the benzene and xylenes were among the main products, while at a W/F = 0.19 g_{cat} h $g_{anisole}^{-1}$ (Figure 9), the phenol was obtained with higher selectivity.

3.5. Analysis of the Reaction Network. The reaction network in Scheme 1 shows that there are three main reactions by which the anisole can be converted:

- Disproportionation, leading to the formation of methylanisole and phenol.
- Demethylation, forming phenol. In this step, the metal is needed to break the O−C bond.
- Isomerization, forming cresol.

Once the phenol is formed, it can be dehydrated on the acid sites or deoxygenated on the metal, forming benzene. The disproportionation requires strong acid sites, and because of this, platinum supported on alumina and on NaH-B are the catalysts that form a higher amount of Ar-OR compounds (see Figure 3). Since Pt/Na−B and Pt/SiO_2 catalysts have weak acid sites in a high proportion, the reactions on the metal sites predominate, forming more benzene as compared to the catalysts that have higher proportion of medium and strong acid sites, such as Pt/γ-Al_2O_3 and Pt/NaH-B catalysts. This behavior is observed at low W/F, such as 0.1 g_{cat} h $g_{anisole}^{-1}$.

The difference in catalytic behavior between pure alumina (section 3.2.1) and the Pt/γ-Al_2O_3 catalyst is quite interesting. While the pure alumina leads only to the formation of oxygenated compounds and deactivated very fast, the addition of Pt led to the formation of deoxygenated compounds and is much more stable (see Figure 3B). It is important also to highlight the fact that on pure alumina, the amount of coke deposited during the reaction is more than double the amount on the Pt/γ-Al_2O_3 catalyst. This is because on Pt, deoxygenated compounds are formed relatively fast, and these compounds do not form as much coke as the oxygenated ones. Scheme 1 shows that if no metal is present, only oxygenated compounds are obtained. On the other hand, as discussed in section 3.2.2, coke is formed mainly from the oxygenated compounds; therefore, the absence of Pt leads to a fast deactivation of the support, while in the presence of the metal the reaction proceeds faster toward the formation of nonoxygenated products, thus improving not only the selectivity, but also the stability.

The temperature has a very strong effect in changing the relative rates of each of the steps shown in Scheme 1, including coke deposition. It is very interesting that with Pt/SiO_2 at low temperature, it is possible to maximize the fraction of aromatics without oxygenated compounds among the products, if the W/F is high enough, for example, 0.8 g_{cat} h $g_{anisole}^{-1}$. A similar result was obtained with the Pt/γ-Al_2O_3 catalyst, obtaining benzene with very high selectivity at 200 °C, and increasing the selectivity to toluene and xylenes at 350 °C. These results suggest that the activation energy for the demethylation reaction is the smaller of those involved in the initial transformation of anisole, and thus, as the temperature is increased, other products increase their production relative to benzene.

3.5.1. Deoxygenation of Anisole: Comparison with m-Cresol. As above-mentioned, the catalysts used in this work have been previously studied in the hydrodeoxygenation of m-cresol.[5−7] To design processes for deoxygenation of real biooils, it is important to determine whether a given catalyst can be used to efficiently deoxygenate different compounds under the same reaction conditions. By using m-cresol as reactant, it was found that high metal/acid sites ratio was required to obtain high levels of toluene yield, with very low selectivity to methane and other light compounds. A faster deactivation was observed at higher density of acid sites, such as in the case of Pt/NaH-B. On the other hand, acid sites with medium and high strength are needed to favor the alkylation of the aromatic ring with the CH_3 fragments formed by demethylation of intermediates compound and coke precursors. Because of this, in the case of the Pt/SiO_2 catalyst, a higher selectivity to light products was observed both with m-cresol and anisole as feed. The optimum temperature found for the deoxygenation of m-cresol on Pt/Al_2O_3 was in the range 300−350 °C, in agreement with the results found in the present study with anisole. Among the catalysts presented in these studies, Pt/Al_2O_3 was the best catalyst regarding a high selectivity and activity toward the production of deoxygenated compounds.

3.6. Catalyst Deactivation and Regeneration. All the catalysts studied presented deactivation due to coke deposition. As seen in Figure 5, the TPO profiles for Pt/SiO_2 catalyst presented two maxima, and the same was observed for all the spent catalysts studied in this work (profiles not shown). These two maxima correspond to carbon deposited on the metal or near the metal particles and on the support, respectively, as observed in the deoxygenation of cresol with the same catalysts studied here.[5−7] It has been found that both the metal and the acid functions are necessary to obtain high activity and selectivity toward the desired products. The study of various carbonaceous deposits formed at different W/F previously discussed suggested that the acid function deactivates faster than the metallic function. This fact was observed by comparing the TPO profiles of spent catalysts used at different space times. Figure 5 shows that at high space time, a higher proportion of the coke is deposited on the acid sites.

On the basis of the results obtained both with cresol and with anisole, to achieve regeneration of the catalyst, it is essential to

DOI: 10.1021/acs.iecr.7b00521
Ind. Eng. Chem. Res. 2017, 56, 6419−6431

recover mainly the metal function. Figure 10 shows cycles of reaction before and after regeneration treatments with air at

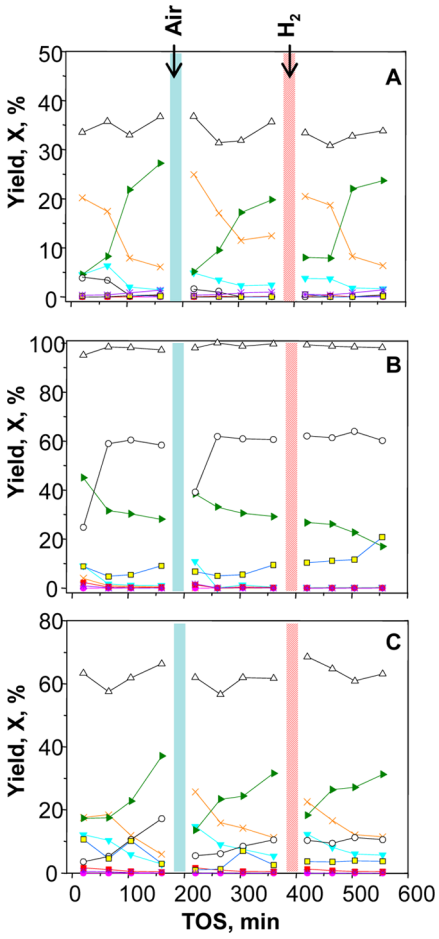

Figure 10. Anisole conversion and product yields versus time on stream before and after regeneration with air at 350−400 °C and after regeneration in H_2 at 500 °C: (A) Pt(1.7)/SiO_2, W/F = 0.02, 300 °C; (B) Pt(1.7)/γ-Al_2O_3 W/F = 0.08, 300 °C; and (C) Pt(1.7)/Na−B W/F = 0.05, 400 °C. References: (open delta) anisole conversion, (orange) LH, (cyan) benzene, (magenta) methylcyclohexane, (red) toluene, (violet) xylenes, (green) phenol, (open circle) Ar-OR, (open square) others.

350 °C and with H_2 at 500 °C for Pt/SiO_2, Pt/γ-Al_2O_3, and Pt/Na−B catalysts. The reaction conditions were: W/F = 0.02 g_{cat} h $g_{anisole}^{-1}$ and 300 °C with Pt/SiO_2, W/F = 0.08 g_{cat} h $g_{anisole}^{-1}$ and 300 °C with Pt/γ-Al_2O_3, and W/F = 0.05 g_{cat} h $g_{anisole}^{-1}$ and 400 °C for Pt/Na−B. In all cases, the H_2/anisole molar ratio was 83. The chosen space time value was low enough to clearly observe the deactivation/regeneration phenomena. Conversion values did not change significantly during the reaction, but the selectivity did change, which demonstrated that deactivation existed during the reaction. For example, the Pt/SiO_2 catalyst (Figure 10A) displays a pronounced change in selectivity to phenol and light compounds as a function of time. In this catalyst, the demethylation reaction and other C−C bond breakage reactions leading to light hydrocarbons are formed mainly on the metallic sites since the acidity is very low. As catalyst deactivates, the more demanding C−C hydrogenolysis deactivates faster and consequently the selectivity to light compounds decreases and to phenol increases.

The first treatment consisted of using air at 350 °C for Pt/SiO_2 and Pt/γ-Al_2O_3, and 400 °C for Pt/Na−B during 1 h until coke represented by the first peak of the TPO was removed. Figure S3 in the Supporting Information shows that effectively the first peak is removed during the treatment at 350 °C and that also a fraction of the coke deposited on the support was eliminated. The results of the regeneration experiments are shown in Figure 10. At these conditions, the regeneration in air was possible with the three catalysts. These results agree with those previously found during the deoxygenation of m-cresol.[7] The TPO profiles shown in Figure 5 indicate that the treatment in air at 350 °C removes the coke from the metal but does not remove all the coke from the support. However, this treatment is enough to restore the activity, showing that the acid function is not controlling the overall reaction rate. In previous publications, it was observed that in the m-cresol deoxygenation with these same catalysts, the regeneration treatment in air led to a change in the metal/acid sites effective ratio since coke was fully removed from the metal particles, but a small amount was left on the support. However, an important conclusion obtained from this study is that it was not necessary to completely regenerate both catalytic functions to recover the activity and that the regeneration of the metallic function is a key factor to regenerate the catalyst with air.

The regeneration treatment in H_2 at 500 °C was possible with Pt/SiO_2 and Pt/Na−B catalysts, but not with Pt/γ-Al_2O_3. In a previews work,[6] dealing with regeneration of these same catalysts but used in the deoxygenation of cresol, the same behavior was observed, that is, the regeneration with air was feasible with all the catalysts but the regeneration in H_2 was possible with Pt/SiO_2 and Pt/Na−B catalysts, but not with Pt/γ-Al_2O_3. The reason that accounted for this behavior in the case of cresol deoxygenation reaction was that the high temperature treatment in hydrogen of Pt/γ-Al_2O_3 catalyst led to the formation of a coke with high toxicity because the coke precursors are polymerized precisely on top of the active sites, thus leading to its deactivation. This led to a decrease of the activity of the acid function in such a way that the catalyst looses the activity for the dehydration step that is needed to obtain toluene. The lack of Brønsted acid sites and the almost exclusive presence of strong Lewis acid sites in the Pt/γ-Al_2O_3 catalyst can be related to the formation of coke with high toxicity.[6,7] This explanation can be extended to anisole deoxygenation because the reactions leading to the products observed in this case also require acidic sites. This same deactivation mechanism during partial regeneration of catalysts, that is, when not all the coke is removed by gasification, was found on zeolite catalysts during isobutene alkylation with C4 olefins.[28]

4. CONCLUSIONS

In this work, anisole deoxygenation with platinum catalysts supported on materials of different acidity was studied. SiO_2, low acid γ-Al_2O_3, and mild acid Na−B and NaH-B materials were used. The metal is responsible for the phenol deoxygenation, while transalkylation reactions like disproportionation, isomerization, and alkylation, as well as condensation reactions are catalyzed by the support acid sites. Anisole demethylation is catalyzed both by metal and acid functions. It is feasible to deoxygenate anisole to benzene with a high selectivity, for example, with Pt/γ-Al_2O_3, W/F = 0.8 g_{cat} h $g_{anisole}^{-1}$, H_2/anisole = 83, and low temperature, approximately 250 °C. Only at certain conditions, that is, at high H_2 partial

DOI: 10.1021/acs.iecr.7b00521
Ind. Eng. Chem. Res. 2017, 56, 6419−6431

pressure and high space time, it is possible to deoxygenate anisole to xylene and benzene. Under moderate reaction conditions, the main deoxygenated product is benzene, produced mainly by metal catalyzed reaction, and only low level of acidity is required in the demethylation primary step. Pt/SiO_2 catalyst is adequate for this reaction. Toluene can also be produced, but it is only observed when acid sites are present in the catalyst, like in the Pt/Na−B catalyst used in this work.

$Pt/\gamma\text{-}Al_2O_3$ catalyst has the highest selectivity to deoxygenated compounds, at rather low temperatures, being this a very important result, although it requires higher values of space time to be selective to deoxygenated products since its acid sites density is low. The Pt/Na−B and even more the Pt/NaH-B catalysts are more selective to oxygenated products (Ar-OR) since their production is favored with higher values of acidity. Therefore, the acidity has to be adjusted to a level enough to catalyze the dehydration reaction without forming large amounts of Ar-OR compounds. The acidity is beneficial also considering that it promotes the alkylation avoiding the carbon lost. Then a rational balance needs to be obtained between production of deoxygenated products and carbon lost. There is an optimal intermediate temperature to obtain deoxygenated products without a significant carbon loss and deactivation by carbon deposits. Finally, the catalysts studied in this work can be regenerated with air at a relatively low temperature.

■ ASSOCIATED CONTENT

Supporting Information

The Supporting Information is available free of charge on the ACS Publications website at DOI: 10.1021/acs.iecr.7b00521.

Detailed data of surface area and pore volumes; XRD spectra, TEM images; TPO of regenerated catalyst (PDF)

■ AUTHOR INFORMATION

Corresponding Author

*E-mail: querini@fiq.unl.edu.ar. Phone: +54-342-4533858. Fax: +54-342-4531068.

ORCID

C. A. Querini: 0000-0003-3057-8770

Notes

The authors declare no competing financial interest.

■ ACKNOWLEDGMENTS

The authors wish to acknowledge the financial support received from ANPCyT (PICT 2012), CONICET (PIP 093), and CAID+D-UNL (PACT 069). Thanks are also given to Diego López Delzar, José Ignacio Lobos, and Claudio Perezlindo for the technical support.

■ REFERENCES

(1) Sheu, Y.-H. E.; Anthony, R. G.; Soltes, E. J. Kinetic studies of upgrading pine pyrolytic oil by hydrotreatment. *Fuel Process. Technol.* **1988**, *19*, 31−50.

(2) Baker, E. G.; Elliott, D. C. Catalytic Upgrading of Biomass Pyrolysis Oils. In *Research in Thermochemical Biomass Conversion*; Bridgwater, A. V., Kuester, J. L., Eds.; Springer: The Netherlands, 1988; pp 883−895.

(3) Agblevor, F.; Besler, S. Inorganic compounds in biomass feedstocks. 1. Effect on the quality of fast pyrolysis oils. *Energy Fuels* **1996**, *10*, 293−298.

(4) Li, K.; Wang, R.; Chen, J. Hydrodeoxygenation of Anisole over Silica-Supported Ni2P, MoP, and NiMoP Catalysts. *Energy Fuels* **2011**, *25*, 854−863.

(5) Zanuttini, M. S.; Lago, C. D.; Querini, C. A.; Peralta, M. A. Deoxygenation of m-cresol on $Pt/\gamma\text{-}Al_2O_3$ catalysts. *Catal. Today* **2013**, *213*, 9−17.

(6) Zanuttini, M. S.; Peralta, M. A.; Querini, C. A. Deoxygenation of m-Cresol: Deactivation and Regeneration of Pt/γ-Al2O3 Catalysts. *Ind. Eng. Chem. Res.* **2015**, *54*, 4929−4939.

(7) Zanuttini, M. S.; Dalla Costa, B. O.; Querini, C. A.; Peralta, M. A. Hydrodeoxygenation of m-cresol with Pt supported over mild acid materials. *Appl. Catal., A* **2014**, *482*, 352−361.

(8) Gonzalez-Borja, M. A.; Resasco, D. E. Anisole and Guaiacol Hydrodeoxygenation over Monolithic Pt−Sn Catalysts. *Energy Fuels* **2011**, *25*, 4155−4162.

(9) Runnebaum, R. C.; Lobo-Lapidus, R. J.; Nimmanwudipong, T.; Block, D. E.; Gates, B. C. Conversion of Anisole Catalyzed by Platinum Supported on Alumina: The Reaction Network. *Energy Fuels* **2011**, *25*, 4776−4785.

(10) Yang, Y.; Ochoa-Hernández, C.; de la Peña O'Shea, V. A.; Pizarro, P.; Coronado, J. M.; Serrano, D. P. Effect of metal−support interaction on the selective hydrodeoxygenation of anisole to aromatics over Ni-based catalysts. *Appl. Catal., B* **2014**, *145*, 91−100.

(11) Khromova, S. A.; Smirnov, A. A.; Bulavchenko, O. A.; Saraev, A. A.; Kaichev, V. V.; Reshetnikov, S. I.; Yakovlev, V. A. Anisole hydrodeoxygenation over Ni−Cu bimetallic catalysts: The effect of Ni/Cu ratio on selectivity. *Appl. Catal., A* **2014**, *470*, 261−270.

(12) Jin, S.; Xiao, Z.; Li, C.; Chen, X.; Wang, L.; Xing, J.; Li, W.; Liang, C. Catalytic hydrodeoxygenation of anisole as lignin model compound over supported nickel catalysts. *Catal. Today* **2014**, *234*, 125−132.

(13) Sankaranarayanan, T. M.; Berenguer, A.; Ochoa-Hernández, C.; Moreno, I.; Jana, P.; Coronado, J. M.; Serrano, D. P.; Pizarro, P. Hydrodeoxygenation of anisole as bio-oil model compound over supported Ni and Co catalysts: Effect of metal and support properties. *Catal. Today* **2015**, *243*, 163−172.

(14) Peters, J. E.; Carpenter, J. R.; Dayton, D. C. Anisole and Guaiacol Hydrodeoxygenation Reaction Pathways over Selected Catalysts. *Energy Fuels* **2015**, *29* (2), 909−916.

(15) Zhu, X.; Lobban, L. L.; Mallinson, R. G.; Resasco, D. E. Bifunctional transalkylation and hydrodeoxygenation of anisole over a Pt/HBeta catalyst. *J. Catal.* **2011**, *281*, 21−29.

(16) Loricera, C. V.; Pawelec, B.; Infantes-Molina, A.; Álvarez-Galván, M. C.; Huirache-Acuña, R.; Nava, R.; Fierro, J. L. G. Hydrogenolysis of anisole over mesoporous sulfided CoMoW/SBA-15(16) catalysts. *Catal. Today* **2011**, *172*, 103−110.

(17) Benson, J.; Hwang, H.; Boudart, M. Hydrogen-oxygen titration method for the measurement of supported palladium surface areas. *J. Catal.* **1973**, *30*, 146−153.

(18) Baerlocher, C.; McCusker, L. B.; Olson, D. H. *Atlas of Zeolite Framework Types*, 6th ed.; E-Publishing via Elservier, 2007.

(19) Meephoka, C.; Chaisuk, C.; Samparnpiboon, P.; Praserthdam, P. Effect of phase composition between nano γ and χ-Al2O3 on Pt/Al2O3 catalyst in CO oxidation. *Catal. Commun.* **2008**, *9*, 546−550.

(20) Tiernan, M. J.; Finlayson, O. E. Effects of ceria on the combustion activity and surface properties of Pt/Al_2O_3 catalysts. *Appl. Catal., B* **1998**, *19*, 23−35.

(21) Santos, A. C. S. F.; Damyanova, S.; Teixeira, G. N. R.; Mattos, L. V.; Noronha, F. B.; Passos, F. B.; Bueno, J. M. C. The effect of ceria content on the performance of $Pt/CeO_2/Al_2O_3$ catalysts in the partial oxidation of methane. *Appl. Catal., A* **2005**, *290*, 123−132.

(22) Taylor, D. R.; Ludlum, K. H. Structure and orientation of phenols chemisorbed on gamma-alumina. *J. Phys. Chem.* **1972**, *76* (20), 2882−2886.

(23) Zhu, X.; Mallinson, R. G.; Resasco, D. E. Role of transalkylation reactions in the conversion of anisole over HZSM-5. *Appl. Catal., A* **2010**, *379*, 172−181.

(24) Nie, L.; Resasco, D. E. Kinetics and mechanism of m-cresol hydrodeoxygenation on a Pt/SiO2 catalyst. *J. Catal.* **2014**, *317*, 22−29.

DOI: 10.1021/acs.iecr.7b00521
Ind. Eng. Chem. Res. 2017, 56, 6419−6431

(25) Nie, L.; de Souza, P. M.; Noronha, F. B.; An, W.; Sooknoi, T.; Resasco, D. E. Selective conversion of m-cresol to toluene over bimetallic Ni−Fe catalysts. *J. Mol. Catal. A: Chem.* **2014**, *388*, 47−55.
(26) Phung, T. K.; Lagazzo, A.; Rivero Crespo, M. A.; Sánchez Escribano, V.; Busca, G. A study of commercial transition aluminas and of their catalytic activity in the dehydration of ethanol. *J. Catal.* **2014**, *311*, 102−113.
(27) Foster, A. J.; Do, P. T.; Lobo, R. F. The synergy of the support acid function and the metal function in the catalytic hydrodeoxygenation of m-cresol. *Top. Catal.* **2012**, *55*, 118−128.
(28) Querini, C. A. Isobutane/butene alkylation: regeneration of solid acid catayst. *Catal. Today* **2000**, *62*, 135−143.

DOI: 10.1021/acs.iecr.7b00521
Ind. Eng. Chem. Res. 2017, 56, 6419−6431